



Brown

Tan

Gray



White

Supersymmetric electroweak corrections to $t\bar{t}h$ associated production at e^+e^- colliders

Xiao-Hong Wu^{1,2*}, Chong Sheng Li^{1†} and Jian Jun Liu^{1‡}

¹Department of Physics, Peking University, Beijing 100871, P. R. China

² CCAST (World Lab.), P.O. Box 8730, Beijing 100080, China

August 1, 2003

Abstract

The electroweak corrections of order $\mathcal{O}(\alpha_{\text{em}}m_{t,b}^2/m_w^2)$ and $\mathcal{O}(\alpha_{\text{em}}m_{t,b}^3/m_w^3)$ to Higgs boson associated production with top quark pair are calculated at e^+e^- colliders in the standard model (SM), the two-Higgs-doublet model (2HDM) and the minimal supersymmetric standard model (MSSM). These corrections are a few percent in general, and in the MSSM they can be over ten percent for favorable parameter values allowing by current precise experiments. The total cross sections including the electroweak corrections get their maximal near $\sqrt{s} = 700\text{GeV}$, and can reach 2.8 fb, 2.7 fb and 2.5 fb in the SM, the 2HDM and the MSSM, respectively.

PACS numbers: 12.60.Fr, 12.60.Jv, 14.80.Bn, 14.80.Cp, 14.65.Ha, 13.66.Fg

*Email: wuxh@th.phy.pku.edu.cn

†Email: csli@pku.edu.cn

‡Email: jjliu@pku.edu.cn

1 Introduction

Higgs mechanism [1] is a milestone to the establishment of Standard Model [2] (SM), where the $SU(2)_L$ Higgs doublet generates electroweak symmetry breaking, gives masses to the weak gauge bosons W^\pm, Z through the kinematic terms of Higgs fields, and gives masses to fermions through Yukawa coupling of Higgs with fermions. In the SM with one $SU(2)_L$ Higgs doublet, there is only one physical scalar Higgs boson left after the electroweak symmetry breaking, the CP even Higgs boson h^{SM} , while in the two-Higgs-doublet model (2HDM) with two $SU(2)_L$ Higgs doublets, there are three neutral and two charged Higgs bosons h, H, A , and H^\pm , of which h and H are CP even and A is CP odd. Due to a fundamental scalar h^{SM} , there exists "hierarchy problem" in the SM, where the Higgs self-energy is quadratic divergent from loop of Dirac fermions, which pulls the Higgs mass to a high cut-off scale [3]. Supersymmetry is introduced to solve this problem, through the cancellation of quadratic divergence in the loops of Higgs self-energy, in which 2HDM of usual type II have to be introduced [4], where one Higgs doublet couples to weak isospin $I = \frac{1}{2}$ fermions, and the other Higgs doublet couples to $I = -\frac{1}{2}$ fermions.

The Search for the Higgs boson is one of major objectives of future high-energy collider, after the discovery of top quark [5]. Great effort has been devoted to this direction to study different properties of the Higgs boson. The direct search of Higgs boson at LEP II through the process $e^+e^- \rightarrow Zh^{\text{SM}}$ has set the lower experimental limit of 114.1GeV on the Standard Model CP even Higgs boson mass [6]. Indirect constraint on the mass of Higgs boson from the W mass measured at Tevatron and LEP II and top quark mass measured at Tevatron is below 195GeV at 95% confidence level [7], which signifies a light Higgs boson. The latest lower limit on the lightest CP-even Higgs boson mass in MSSM is $m_h \geq 91.0\text{GeV}$ [8, 9], where production process $e^+e^- \rightarrow Zh$ is suppressed with small $\sin^2(\beta - \alpha)$. When $\sin^2(\beta - \alpha)$ is not suppressed, the limit on the lightest CP-even Higgs boson mass from above process is about 114GeV [9] in the MSSM. While in the MSSM, because supersymmetry relates Higgs quadratic coupling to the gauge coupling, there exists an upper limit on the lightest CP-even Higgs boson mass $m_h \leq 130\text{GeV}$ [10] when including radiative corrections.

With a heavy top quark, $t\bar{t}h$ associated production also can be helpful for both the discovery of a Higgs boson in the intermediate mass range and the measurement of large top quark Yukawa coupling at the near future colliders. There are the possibilities at the Tevatron Run II to search the Higgs boson through $q\bar{q} \rightarrow t\bar{t}h$ production subprocess, followed by $h \rightarrow b\bar{b}$, for $m_h \leq 140\text{GeV}$ [11], though the statistics are too low to measure $t\bar{t}h$ Yukawa coupling. At the CERN Large Hadron Collider (LHC), the process $pp \rightarrow t\bar{t}h$ is an important search channel for a light Higgs mass from 100GeV to 130GeV [12], and the statistics will allow a measurement of $t\bar{t}h$ Yukawa coupling at 11.9% level with $m_h = 120\text{GeV}$ [13]. Recently, at the Tevatron and the LHC, $\mathcal{O}(\alpha_s)$ QCD corrections to $t\bar{t}h$ production processes have been investigated in Ref. [14, 15]. At e^+e^- colliders, the measurement of the $t\bar{t}h$ Yukawa coupling can be significantly improved through the process $e^+e^- \rightarrow t\bar{t}h$. With integrated luminosity of 1000fb^{-1} , at $\sqrt{s} = 500\text{GeV}$, the top Yukawa coupling can be measured at an accuracy of $\delta g_{t\bar{t}h}/g_{t\bar{t}h} \simeq 21\%$, and with integrated luminosity of 500fb^{-1} , at $\sqrt{s} = 800\text{GeV}$, the measurement of top Yukawa coupling can reach the level of $\delta g_{t\bar{t}h}/g_{t\bar{t}h} \simeq 5\%$ [16]. As shown in Ref. [17] that since the $t\bar{t}h$ Yukawa coupling can be significantly different in the supersymmetric (SUSY) model from one in the SM, the measurement would provide a mean of discriminating between models. Thus the theoretical predictions including higher-order quantum effects in the different models, which also enters into the rate and dilutes the interpretation of the signal as the measurement of the $t\bar{t}h$ coupling, should be important. At e^+e^- linear colliders, $t\bar{t}h$ associated production process was discussed at tree-level many years ago [18], and its QCD corrections were also given in Ref. [17]. Very recently, a calculation of the SUSY-QCD corrections to the process has been presented in Ref. [19]. In this paper, we present the calculation of the $\mathcal{O}(\alpha_{\text{em}} m_{t,b}^2/m_w^2)$ and $\mathcal{O}(\alpha_{\text{em}} m_{t,b}^3/m_w^3)$ electroweak corrections in the SM, the 2HDM of type II, and the MSSM.

The paper is arranged as follow. In section 2, we present the notation and analytical calculations. In section 3, we give our numerical results and discussions. our conclusions are given in section 4. The lengthy explicit expressions of the irreducible self-energies and vertices are given in the Appendix.

2 Evaluation

2.1 Formalism

Firstly, we define the kinematical variables and list a compact formula for the one-loop virtual corrections to $e^-e^+ \rightarrow t\bar{t}h$. The momenta of incoming electron e^- and positron e^+ are p_1 and p_2 , respectively, and the momenta of outgoing top quark t , anti-top quark \bar{t} and the Higgs boson h are assigned to k_1 , k_2 and k_3 correspondingly, with the center of mass energy squared $s = (p_1 + p_2)^2 = (k_1 + k_2 + k_3)^2$, for the process

$$e^-(p_1) + e^+(p_2) \rightarrow t(k_1) + \bar{t}(k_2) + h(k_3). \quad (1)$$

Because of the smallness of electron mass, we neglect Higgs-electron-electron Yukawa coupling, the $2 \rightarrow 3$ process (1) can be split to two parts: the electron and positron are annihilated to time-like γ and Z , and then the virtual γ, Z decay to $t\bar{t}h$ final states. Therefore, the differential cross section of the process (1) with averaged over spin of incoming states and summed over spin and color of outgoing states can be simplified, which should only depend on two parameters, conveniently chosen as the energy of outgoing top quark k_1^0 , and the energy of outgoing Higgs boson k_3^0 , and the differential cross section including the one-loop virtual corrections can be written in the general form

$$\frac{d\sigma}{dk_3^0 dk_1^0} = \frac{N_c}{4} \frac{1}{8(2\pi)^4} \frac{1}{2s} \sum_{\text{spins}} [|M^{\text{tree}}|^2 + 2\text{Re}(M^{\text{tree}} \delta M^+)], \quad (2)$$

where N_c is the $SU(3)_c$ color factor, M^{tree} is tree level amplitude, and δM is the one-loop corrections to the tree-level process, which contain the irreducible corrections $\delta M_{\text{irr}}^{(\text{self}, \text{vertex}, \text{box})}$ and the corresponding counterterms $\delta M_{\text{ct}}^{(\text{self}, \text{vertex})}$:

$$\delta M = \delta M^{\text{self}} + \delta M^{\text{vertex}} + \delta M_{\text{irr}}^{\text{box}} \quad (3)$$

with

$$\begin{aligned} \delta M^{\text{self}} &= \delta M_{\text{irr}}^{\text{self}} + \delta M_{\text{ct}}^{\text{self}}, \\ \delta M^{\text{vertex}} &= \delta M_{\text{irr}}^{\text{vertex}} + \delta M_{\text{ct}}^{\text{vertex}}. \end{aligned} \quad (4)$$

2.2 SUSY electroweak corrections

The SUSY electroweak corrections of order $\mathcal{O}(\alpha_{\text{em}} m_{t,b}^2/m_w^2)$ and $\mathcal{O}(\alpha_{\text{em}} m_{t,b}^3/m_w^3)$ to process (1) arise from the Feynman diagrams shown in **Fig. 1**. We carried out the calculation in the 't Hooft-Feynman gauge and used dimensional reduction to control all the ultraviolet divergences in the virtual loop corrections utilizing the on-mass-shell renormalization scheme [21, 22]. FeynCalc [20] is used to calculate the one-loop irreducible diagrams.

The relevant field renormalization constants are defined as

$$\begin{aligned} t_{L0} &= (1 + \frac{1}{2}\delta Z_L^t) t_L, & t_{R0} &= (1 + \frac{1}{2}\delta Z_R^t) t_R, \\ \begin{pmatrix} Z_\mu \\ A_\mu \end{pmatrix}_0 &= \begin{pmatrix} 1 + \frac{1}{2}\delta Z_{zz} & \frac{1}{2}\delta Z_{z\gamma} \\ \frac{1}{2}\delta Z_{\gamma z} & 1 + \frac{1}{2}\delta Z_{\gamma\gamma} \end{pmatrix} \begin{pmatrix} Z_\mu \\ A_\mu \end{pmatrix}, \\ \begin{pmatrix} H \\ h \end{pmatrix}_0 &= \begin{pmatrix} 1 + \frac{1}{2}\delta Z_{HH} & \frac{1}{2}\delta Z_{Hh} \\ \frac{1}{2}\delta Z_{hH} & 1 + \frac{1}{2}\delta Z_{hh} \end{pmatrix} \begin{pmatrix} H \\ h \end{pmatrix}, \\ \begin{pmatrix} A \\ G \end{pmatrix}_0 &= \begin{pmatrix} 1 + \frac{1}{2}\delta Z_{AA} & \frac{1}{2}\delta Z_{AG} \\ \frac{1}{2}\delta Z_{GA} & 1 + \frac{1}{2}\delta Z_{GG} \end{pmatrix} \begin{pmatrix} A \\ G \end{pmatrix}. \end{aligned} \quad (5)$$

The mass renormalization constants are defined as

$$\begin{aligned}
m_{w0}^2 &= m_w^2 + \delta m_w^2, & m_{z0}^2 &= m_z^2 + \delta m_z^2, \\
m_{t0} &= m_t + \delta m_t, \\
m_{h0}^2 &= m_h^2 + \delta m_h^2, \\
m_{H0}^2 &= m_H^2 + \delta m_H^2, \\
m_{A0}^2 &= m_A^2 + \delta m_A^2.
\end{aligned} \tag{6}$$

As for the CP-even Higgs mixing angle α and $\tan\beta \equiv v_2/v_1$, the ratio of two vacuum expectation values of neutral Higgs fields, they have to be renormalized, too. We defined

$$\begin{aligned}
\alpha_0 &= (1 + \delta Z_\alpha)\alpha, \\
(\tan\beta)_0 &= (1 + \delta Z_\beta)\tan\beta,
\end{aligned} \tag{7}$$

where α and β are not independent in the MSSM.

Below we described in detail the renormalization constants and counterterms in the 2HDM and the MSSM, while ones in the SM can be obtained using standard techniques [22]. For the Higgs sector of the MSSM, using the results of Ref. [23], the relevant renormalization constants are given by

$$\begin{aligned}
\delta m_h^2 &= \Sigma^{hh}(m_h^2) - T_{hh}, \\
\delta m_H^2 &= \Sigma^{HH}(m_H^2) - T_{HH}, \\
\delta Z_{hh} &= -\frac{\partial \Sigma^{hh}(k^2)}{\partial k^2} \Big|_{k^2=m_h^2}, \\
\delta Z_{HH} &= -\frac{\partial \Sigma^{HH}(k^2)}{\partial k^2} \Big|_{k^2=m_H^2}, \\
\delta Z_{hH} &= -2 \frac{\Sigma^{Hh}(m_H^2) - T_{Hh}}{m_H^2 - m_h^2}, \\
\delta Z_{Hh} &= 2 \frac{\Sigma^{Hh}(m_h^2) - T_{Hh}}{m_H^2 - m_h^2}, \\
\delta m_A &= \Sigma^{AA}(m_A^2) - T_{AA}, \\
\delta Z_{AA} &= -\frac{\partial \Sigma^{AA}(k^2)}{\partial k^2} \Big|_{k^2=m_A^2}, \\
\delta Z_{GG} &= -\frac{\partial \Sigma^{GG}(k^2)}{\partial k^2} \Big|_{k^2=0}, \\
\delta Z_{GA} &= -2 \frac{\Sigma^{AG}(m_A^2) - T_{AG}}{m_A^2}, \\
\delta Z_{AG} &= 2 \frac{\Sigma^{AG}(0) - T_{AG}}{m_A^2},
\end{aligned} \tag{8}$$

where the Higgs tadpole parameters $T_h, T_H, T_{HH}, T_{Hh}, T_{hh}, T_{AA}, T_{AG}, T_{GG}, T_{H-H-}, T_{H-G-},$ and T_{G-G-} defined as in Ref. [23]. The renormalization of CP-even Higgs mixing angle α is fixed by [24]

$$\delta Z_\alpha = \frac{1}{4}(\delta Z_{Hh} - \delta Z_{hH}). \tag{9}$$

The renormalization of $\tan\beta$ is fixed by keeping the on-shell $H^+\bar{\tau}\nu_\tau$ coupling the same form to all orders in perturbative series [25], which can be expressed as

$$\delta Z_\beta = \frac{1}{2} \tan\beta \left(\frac{\delta m_w^2}{m_w^2} - \frac{\delta m_z^2}{m_z^2} + \frac{\delta m_z^2 - \delta m_w^2}{m_z^2 - m_w^2} - \delta Z_{H-H-} + \delta Z_{G-H-} \cot\beta \right) \tag{10}$$

with

$$\begin{aligned}
\delta Z_{H^-H^-} &= -\frac{\partial \Sigma^{H^-H^-}(k^2)}{\partial k^2} \Big|_{k^2=m_{H^-}^2}, \\
\delta Z_{G^-H^-} &= -2 \frac{\Sigma^{H^-G^-}(m_{H^-}^2) - T_{H^-G^-}}{m_{H^-}^2}.
\end{aligned} \tag{11}$$

Using above the renormalization constants, for the process (1), the counterterms of Higgs self-energy can be expressed as

$$\begin{aligned}
C_{hh} &= i[k^2 \delta Z_{hh} - m_h^2 \delta Z_{hh} - \delta m_h^2 + T_{hh}], \\
C_{HH} &= i[k^2 \delta Z_{HH} - m_H^2 \delta Z_{HH} - \delta m_H^2 + T_{HH}], \\
C_{hH} &= i[\frac{1}{2}(\delta Z_{hH} + \delta Z_{Hh})k^2 - \frac{1}{2}(m_h^2 \delta Z_{hH} + m_H^2 \delta Z_{Hh}) + T_{hH}], \\
C_{GG} &= i[\delta Z_{GG}k^2 + T_{GG}], \\
C_{AA} &= i[k^2 \delta Z_{AA} - m_A^2 \delta Z_{AA} - \delta m_A^2 + T_{AA}], \\
C_{AG} &= i[\frac{1}{2}(\delta Z_{AG} + \delta Z_{GA})k^2 - \frac{1}{2}m_A^2 \delta Z_{AG} + T_{AG}].
\end{aligned} \tag{12}$$

The counterterms of gauge boson and CP-odd scalar mixing, $Z_\mu - G$ and $Z_\mu - A$ are given by

$$\begin{aligned}
C_{zG} &= k_\mu m_z [\frac{\delta m_z^2}{2m_z^2} + \frac{\delta Z_{zz}}{2} + \frac{\delta Z_{GG}}{2}], \\
C_{zA} &= k_\mu m_z \frac{\delta Z_{GA}}{2}.
\end{aligned} \tag{13}$$

The counterterms of gauge boson and top pair interactions, $\gamma t\bar{t}$ and $Zt\bar{t}$ are given by

$$\begin{aligned}
C_{\gamma tt} &= [g_{tt\gamma}^L (\frac{\delta Z_{\gamma\gamma}}{2} + \delta Z_L^t) + g_{ttz}^L \frac{\delta Z_{z\gamma}}{2} + g_{tt\gamma}^L \frac{\delta e}{e}] \gamma_\mu P_L + (L \rightarrow R), \\
C_{ztt} &= [g_{ttz}^L (\frac{\delta Z_{zz}}{2} + \delta Z_L^t) + g_{tt\gamma}^L \frac{\delta Z_{\gamma z}}{2} + g_{ttz}^L (\frac{\delta e}{e} + \frac{8s_w \delta s_w}{4s_w^2 - 3} - \frac{\delta s_w}{s_w} - \frac{\delta c_w}{c_w})] \gamma_\mu P_L + (L \rightarrow R),
\end{aligned} \tag{14}$$

where $P_{L,R} = (1 \mp \gamma_5)/2$, and $\delta e/e$ is absent at the order of $\mathcal{O}(\alpha_{em} m_{t,b}^2/m_w^2)$ corrections.

The counterterms of Higgs and top pair Yukawa interactions, htt , $Gt\bar{t}$ and $At\bar{t}$ are given by

$$\begin{aligned}
C_{htt} &= [g_{tth}^L (\frac{\delta Z_{hh}}{2} + \frac{\delta Z_t^L}{2} + \frac{\delta Z_t^R}{2}) + g_{tth}^L (\frac{\delta m_t}{m_t} + \frac{\delta e}{e} - \frac{\delta m_w^2}{2m_w^2} - \frac{\delta s_w}{s_w} - \frac{\delta \sin \beta}{\sin \beta} + \frac{\delta \cos \alpha}{\cos \alpha}) + \\
&\quad g_{tth}^L \frac{\delta Z_{Hh}}{2}] P_L + (L \rightarrow R), \\
C_{Gtt} &= [g_{ttG}^L (\frac{\delta Z_{GG}}{2} + \frac{\delta Z_t^L}{2} + \frac{\delta Z_t^R}{2}) + g_{ttG}^L (\frac{\delta m_t}{m_t} + \frac{\delta e}{e} - \frac{\delta m_w^2}{2m_w^2} - \frac{\delta s_w}{s_w}) + \\
&\quad g_{ttA}^L \frac{\delta Z_{AG}}{2}] P_L + (L \rightarrow R), \\
C_{Att} &= [g_{ttA}^L (\frac{\delta Z_{AA}}{2} + \frac{\delta Z_t^L}{2} + \frac{\delta Z_t^R}{2}) + g_{ttA}^L (\frac{\delta m_t}{m_t} + \frac{\delta e}{e} - \frac{\delta m_w^2}{2m_w^2} - \frac{\delta s_w}{s_w} - \frac{\delta \cot \beta}{\cot \beta}) + \\
&\quad g_{ttG}^L \frac{\delta Z_{GA}}{2}] P_L + (L \rightarrow R).
\end{aligned} \tag{15}$$

Note that g_{tti}^L ($i = \gamma, H, h, A, G, Z$) appeared above are the coupling constants.

The counterterms of Higgs and gauge boson pair interactions, $h\gamma\gamma$, $h\gamma z$ and hzz are given by

$$\begin{aligned}
C_{h\gamma\gamma} &= 0, \\
C_{h\gamma z} &= g_{zzh} \frac{\delta Z_{z\gamma}}{2} g_{\mu\nu}, \\
C_{hzz} &= [g_{zzh} (\frac{\delta Z_{hh}}{2} + \delta Z_{zz}) + g_{zzh} (\frac{\delta g}{g} + \frac{\delta m_w^2}{2m_w^2} - 2\frac{\delta c_w}{c_w} + \frac{\delta \sin(\beta - \alpha)}{\sin(\beta - \alpha)}) + g_{zzH} \frac{\delta Z_{Hh}}{2}] g_{\mu\nu}. \quad (16)
\end{aligned}$$

The counterterms of gauge boson and Higgs pair interactions, γhG , γhA , ZhG and ZhA are given by

$$\begin{aligned}
C_{\gamma hG} &= g_{hGz} \frac{\delta Z_{z\gamma}}{2} (k_h - k_G)_\mu, \\
C_{\gamma hA} &= g_{hAz} \frac{\delta Z_{z\gamma}}{2} (k_h - k_A)_\mu, \\
C_{zhG} &= [g_{hGz} (\frac{\delta Z_{zz}}{2} + \frac{\delta Z_{GG}}{2} + \frac{\delta Z_{hh}}{2}) + g_{hGz} (\frac{\delta e}{e} - \frac{\delta c_w}{c_w} - \frac{\delta s_w}{s_w} + \frac{\delta \sin(\beta - \alpha)}{\sin(\beta - \alpha)}) + \\
&\quad g_{hAz} \frac{\delta Z_{AG}}{2} + g_{HGz} \frac{\delta Z_{Hh}}{2}] (k_h - k_G)_\mu, \\
C_{zhA} &= [g_{hAz} (\frac{\delta Z_{zz}}{2} + \frac{\delta Z_{AA}}{2} + \frac{\delta Z_{hh}}{2}) + g_{hAz} (\frac{\delta e}{e} - \frac{\delta c_w}{c_w} - \frac{\delta s_w}{s_w} + \frac{\delta \cos(\beta - \alpha)}{\cos(\beta - \alpha)}) + \\
&\quad g_{hGz} \frac{\delta Z_{GA}}{2} + g_{HAz} \frac{\delta Z_{Hh}}{2}] (k_h - k_A)_\mu. \quad (17)
\end{aligned}$$

With all the counterterms fixed as above, the renormalized amplitude for the process (1) is obtained by adding the counterterms to the corresponding irreducible corrections arising from the self-energy diagrams shown in **Fig. 2 – 6**, the vertex diagrams shown in **Fig. 7 – 10**, and the box diagrams shown in **Fig. 11**, respectively, which can be reduced by FeynCalc [20] and the relevant explicit expressions are given in the Appendix. Using above results it is straightforward to calculate the $\mathcal{O}(\alpha_{\text{em}} m_{t,b}^2/m_w^2)$ and $\mathcal{O}(\alpha_{\text{em}} m_{t,b}^3/m_w^3)$ SUSY electroweak corrections to process (1).

3 Numerical results and Discussion

In this section we present some numerical results. In the SM and the 2HDM, we limit the lightest CP-even Higgs boson mass m_h larger than 114GeV, while in the 2HDM of type II, the lower bound of the charged Higgs boson mass is 350GeV from the constraint of $\text{Br}(B \rightarrow X_s \gamma)$ [26]. In the MSSM, we use SUBHPOLE [27] to calculate the radiative corrections to the CP-even Higgs pole masses and mixing angle α , and the CP-odd Higgs pole mass, which incorporates the one-loop effective potential and two-loop leading-log contributions from arbitrary off-diagonal stop and sbottom matrices. The inclusion of the radiative corrections in the Higgs sector is essential for Higgs phenomenology, because the tree-level lightest CP-even Higgs mass $m_h < m_z$ has been excluded by LEP experiments. There is $\pm 3\text{GeV}$ inaccuracy in SUBHPOLE to calculate the lightest CP-even Higgs boson mass, due to unclear subleading-log and uncalculated higher order corrections, so we take the lower limit of m_h as 111GeV. We also take the lower bound of other SUSY particle masses as, $m_{\tilde{\chi}_1^0} \geq 37\text{GeV}$, $m_{\tilde{\chi}_1^\pm} \geq 94\text{GeV}$, $m_{\tilde{t}_1} \geq 95\text{GeV}$, $m_{\tilde{b}_1} \geq 91\text{GeV}$ [28], and $\Delta\rho \leq 3 \times 10^{-3}$ [29]. In the MSSM, for simplicity, we assume $A_t = A_b$ and use the relation of gaugino masses $M_2 = 2M_1$ at the electroweak scale. In all the three different models, the SM, the 2HDM and the MSSM, there are common features that the contribution of γ exchange channel is dominant in the center of mass energy \sqrt{s} region from 0.5TeV to 1TeV, while the contribution of Z exchange channel increase with increasing \sqrt{s} .

The results in the SM are shown in **Fig. 12** and **Fig. 15**. We present the cross section σ and SUSY electroweak corrections to the cross sections relative to the tree-level values $\Delta\sigma/\sigma^{\text{tree}}$ with $\Delta\sigma \equiv \sigma^{\text{all}} - \sigma^{\text{tree}}$ as a function of the center of mass energy \sqrt{s} with $m_h = 115\text{GeV}$ in **Fig. 15**. The corrections are at most a few percent and decrease with increasing \sqrt{s} . **Fig. 12** gives the cross section and the corrections as a function of the Higgs

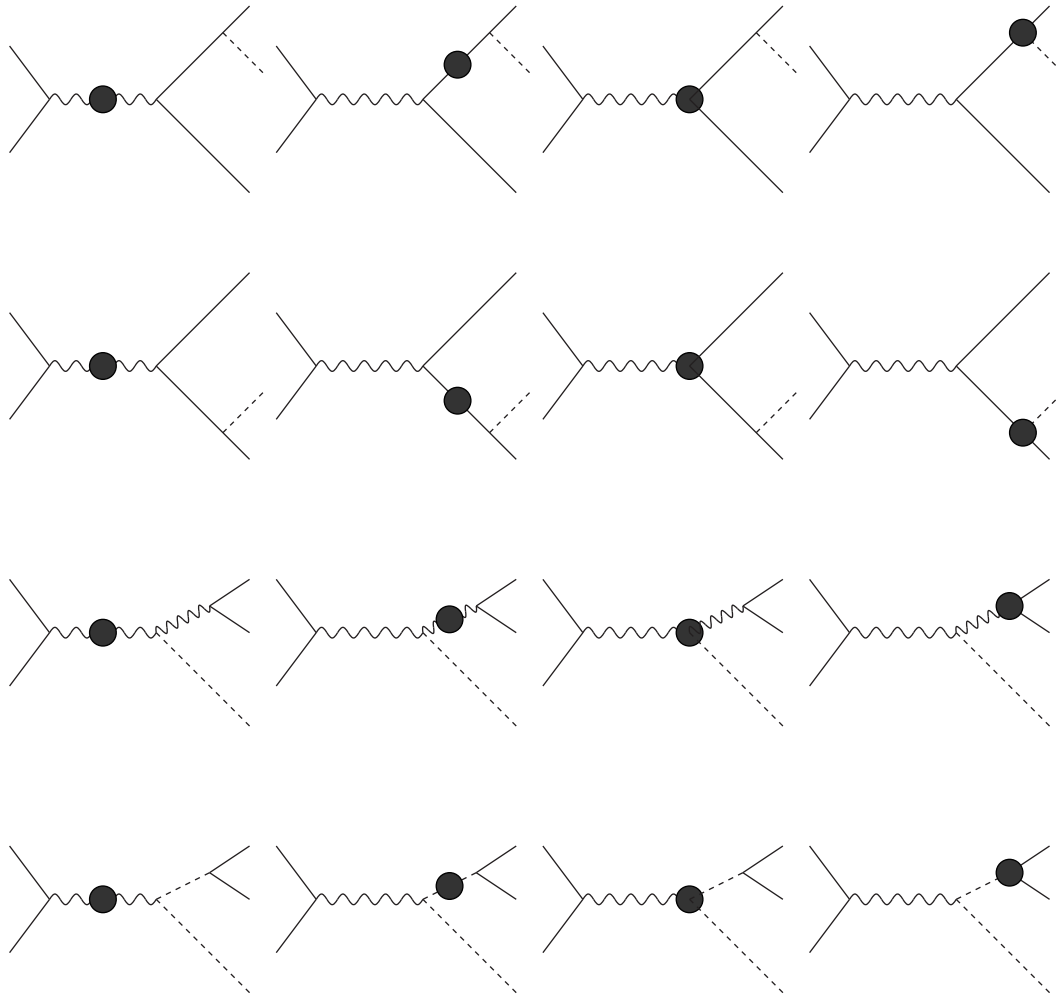


Figure 1: One-loop corrected diagrams of process $e^+e^- \rightarrow t\bar{t}h$.

boson mass m_h at $\sqrt{s} = 800\text{GeV}$. The corrections increase as m_h increase, but still only a few percent. And we can see that the corrections are positive when \sqrt{s} varies from 0.5TeV to 1TeV for $m_h = 115\text{GeV}$ in the SM.

Fig. 13 and **Fig. 15** shows the results in the 2HDM. **Fig. 15** gives σ and $\Delta\sigma/\sigma^{\text{tree}}$ as a function of \sqrt{s} for $\tan\beta = 10$ and $\alpha = 0.05$, assuming $m_h = 115\text{GeV}$, $m_H = 250\text{GeV}$, $m_A = 300\text{GeV}$ and $m_{H^\pm} = 350\text{GeV}$. The corrections imply a few percent reduction in the cross sections, and the magnitude of the corrections firstly increase as \sqrt{s} increase, then slowly decrease. **Fig. 13a** shows the dependence of σ and $\Delta\sigma/\sigma^{\text{tree}}$ on m_h for $\tan\beta = 10$ and $\alpha = 0.05$, assuming $m_H = 300\text{GeV}$, $m_A = 300\text{GeV}$ and $m_{H^\pm} = 300\text{GeV}$. The corrections are negative, and their magnitude can exceed ten percent which increase as m_h increase. In **Fig. 13b**, we present σ and $\Delta\sigma/\sigma^{\text{tree}}$ as a function of $\tan\beta$ for $\alpha = 0.05$, assuming $m_h = 115\text{GeV}$, $m_H = 250\text{GeV}$, $m_A = 300\text{GeV}$ and $m_{H^\pm} = 350\text{GeV}$. The corrections are about 2% reduction in the cross sections, and not sensitive to the values of $\tan\beta$.

In **Fig. 14 – 15**, we give the results in the MSSM. **Fig. 14a** shows the dependence of σ and $\Delta\sigma/\sigma^{\text{tree}}$ on μ for $\tan\beta = 44$, assuming $m_A = 308\text{GeV}$, $M_1 = 59\text{GeV}$, $A_t = 562\text{GeV}$ and $m_{\tilde{t}_R} = m_{\tilde{b}_R} = m_{\tilde{q}} = 375\text{GeV}$. The total cross section σ only slightly depend on the μ , but has a strong dependence on the c.m. energy \sqrt{s} , as shown in **Fig. 14a** (left); the magnitude of the corrections $\Delta\sigma/\sigma^{\text{tree}}$ is a few percent in general, and can exceed 10% for $\mu > 700\text{ GeV}$, as shown in **Fig. 14a** (right). **Fig. 14b** exhibits σ and $\Delta\sigma/\sigma^{\text{tree}}$ as a function of the lightest scalar top quark mass $m_{\tilde{t}_1}$ for $\tan\beta = 4, 10$ and 40, respectively, with $m_A = 250\text{GeV}$, $\mu = 220\text{GeV}$, $M_1 = 65\text{GeV}$, $A_t = 1100\text{GeV}$, and $m_{\tilde{t}_R} = m_{\tilde{b}_R} = 1.3m_{\tilde{q}}$. One can see that the results are not sensitive to the values of $\tan\beta$, where there is a cut in the curve for $\tan\beta = 4$ with $m_{\tilde{t}_1}$ below 180GeV due to the constraint of the lightest CP-even Higgs mass lower bound as shown in **Fig. 14b** (left). With $\sqrt{s} = 800\text{GeV}$, the corrections decrease the cross sections, and their magnitudes become smaller with $m_{\tilde{t}_1}$ increasing, but with $\sqrt{s} = 500\text{GeV}$, the corrections can increase or decrease the cross sections depending on $m_{\tilde{t}_1}$, and they are less than a few percent in general, however, when $m_{\tilde{t}_1}$ is below 110GeV, the corrections can be over -10% with $\sqrt{s} = 800\text{GeV}$ as shown in **Fig. 14b** (right). We show σ and $\Delta\sigma/\sigma^{\text{tree}}$ as a function of \sqrt{s} in **Fig. 15** for $\tan\beta = 6$ and 40, respectively, with $m_A = 160\text{GeV}$, $\mu = 220\text{GeV}$, $M_1 = 70\text{GeV}$, $A_t = 1000\text{GeV}$, and $m_{\tilde{t}_R} = m_{\tilde{b}_R} = 1.5m_{\tilde{q}}$. The corrections decrease the cross sections, and their magnitudes increase as \sqrt{s} increasing, which range between $0 \sim 8\%$ and $4\% \sim 13\%$ for $\tan\beta = 6$ and $\tan\beta = 40$, respectively.

4 Conclusion

To summarize, we have calculated the electroweak corrections of order $\mathcal{O}(\alpha_{\text{em}}m_{t,b}^2/m_w^2)$ and $\mathcal{O}(\alpha_{\text{em}}m_{t,b}^3/m_w^3)$ to process $e^+e^- \rightarrow t\bar{t}h$ in the SM, the 2HDM and the MSSM, respectively. These corrections are a few percent in general, and can be over 10% in the MSSM with the lightest scalar top and bottom quark mass near the lower bound. The total cross sections including the electroweak corrections for process $e^+e^- \rightarrow t\bar{t}h$ get their maximal near $\sqrt{s} = 700\text{GeV}$, and can reach 2.8 fb, 2.7 fb and 2.5 fb in the SM, the 2HDM and the MSSM, respectively.

Note added: While preparing this manuscript three papers [31, 32, 33] appeared where the electroweak corrections to the same process in the SM are also calculated, the numerical results of their virtual weak corrections are in agreement with our results in the case of the SM.

Acknowledgments

One of the authors X.-H.W. would like to thank Dr. Shou-Hua Zhu for his generous discussion about numerical calculations.

References

- [1] P. W. Higgs, Phys. Lett. **12** (1964) 132; Phys. Rev. Lett. **13** (1964) 508; Phys. Rev. **145** (1966) 1156; F. Englert and R. Brout, Phys. Rev. Lett. **13** (1964) 321; G. S. Guralnik, C. R. Hagen and T. W. Kibble, Phys. Rev. Lett. **13** (1964) 585; T. W. Kibble, Phys. Rev. **155** (1967) 1554.

- [2] S. L. Glashow, Nucl. Phys. **22** (1961) 508; S. Weinberg, Phys. Rev. Lett. **19** (1967) 1264; A. Salam, in Proceedings of the Eighth Nobel Symposium, edited by N. Svartholm (Almqvist and Wiksell, Stockholm, 1968; Wiley, New York, 1978), p367.
- [3] S. Weinberg, Phys. Rev. **D13** (1976) 974; Phys. Rev. **D19** (1979) 1277; L. Susskind, Phys. Rev. **D20** (1979) 2619; G. 't Hooft, in **Recent developments in gauge theories**, Proceedings of the NATO Advanced Summer Institute, Cargese 1979, ed. G. 't Hooft et. al. (Plenum, New York 1980).
- [4] J. F. Gunion, H. E. Haber, G. L. Kane and S. Dawson, The Higgs Hunter's Guide, Addison-Wesley, 1990.
- [5] CDF Collaboration, F. Abe, et. al., Phys. Rev. Lett. **74** (1995) 2626; D0 Collaboration, F. Abachi, et. al., Phys. Rev. Lett. **74** (1995) 2632.
- [6] LEP Higgs Working Group, arXiv:hep-ex/0107029.
- [7] LEP Electroweak Working Group, LEPEWWG/2002-01, May 8, 2002.
- [8] LEP Higgs Working Group, arXiv:hep-ex/0107030, arXiv:hep-ex/0107031.
- [9] A. Sopczak, arXiv:hep-ph/0112082, arXiv:hep-ph/0112086.
- [10] Y. Okada, M. Yamaguchi and T. Yanagida, Prog. Theor. Phys. **85** (1991)1; H. Haber and R. Hempfling, Phys. Rev. Lett. **66** (1991) 1815; J. Ellis, G. Ridolfi and F. Zwirner, Phys. Lett. **B257** (1991) 83; J. Ellis, G. Ridolfi and F. Zwirner, Phys. Lett. **B262** (1991) 477; R. Barbieri, F. Caravaglios and M. Frigeni, Phys. Lett. **B258** (1991) 167; R. Hempfling and A. Hoang, Phys. Lett. **B331** (1994) 99; J. A. Casas, J. R. Espinosa, M. Quiros and A. Riotto, Nucl. Phys. **B436** (1995) 3; M. Carena, J. R. Espinosa, M. Quiros and C. Wagner, Phys. Lett. **B355** (1995) 209; H. Haber, R. Hempfling and A. Hoang, Z. Phys. **C75** (1997) 539.
- [11] J. Goldstein, C. S. Hill, J. Incandela, S. Parke, D. Rainwater, D. Stuart, Phys. Rev. Lett. **86** (2001) 1694.
- [12] E. Richter-Was and M. Sapinski, Acta Phys. Polon. **B30** (1999) 1001; V. Drollinger, T. Muller, D. Denecri, arXiv:hep-ph/0111312; F. Maltoni, D. Rainwater, S. Willenbrock, Phys. Rev. **D66** (2002) 034022; A. Belyaev and L. Reina, JHEP **0208** (2002) 041; T. Abe *et al.*, arXiv:hep-ex/0106056.
- [13] For a review, see M. Beneke *et al.*, arXiv:hep-ph/0003033.
- [14] W. Beenakker, S. Dittmaier, M. Kramer, B. Plumper, M. Spira and P. M. Zerwas, Phys. Rev. Lett. **87** (2001) 201805; Nucl. Phys. **B653** (2003) 151.
- [15] L. Reina and S. Dawson, Phys. Rev. Lett. **87** (2001) 201804; S. Dawson, C. Jackson, L. H. Orr, L. Reina, D. Wackerroth, arXiv:hep-ph/0305087.
- [16] J. F. Gunion, B. Grzadkowski and X. -H. He, Phys. Rev. Lett. **77** (1996) 5172; S. Dawson and L. Reina, Phys. Rev. **D57** (1998) 5851; Phys. Rev. **D59** (1999) 054012; S. Dawson and L. Reina, Phys. Rev. **D60** (1999) 015003; A. Juste and G. Merino, arXiv:hep-ph/9910301; H. Baer, S. Dawson, and L. Reina, Phys. Rev. **D61** (2000) 013002; and J. F. Gunion, H. E. Haber, R. V. Kooten, arXiv:hep-ph/0301023 for a recent review.
- [17] S. Dittmaier, M. Kramer, Y. Liao, M. Spira and P. M. Zerwas, Phys. Lett. **B441** (1998) 383; S. Dawson, and L. Reina, Phys. Rev. **D59** (1999) 054012; S. Dawson, and L. Reina, Phys. Rev. **D60** (1999) 015003; S. Dittmaier, M. Kramer, Y. Liao, M. Spira and P. M. Zerwas, Phys. Lett. **B478** (2000) 247.
- [18] K. J. F. Gaemers and G. J. Gounaris, Phys. Lett. **B77** (1978) 379; A. Djouadi, J. Kalinowski and P. M. Zerwas, Zeit. Phys. **C54** (1992) 255.
- [19] S. -H. Zhu, arXiv:hep-ph/0212273.

- [20] G. Passarino and M. Veltman, Nucl. Phys, **B160** (1979) 151; R. Mertig, M. Bohm, and A. Denner, Comp. Phys. Comm. **64** (1991) 345.
- [21] S. Sirlin, Phys. Rev. **D22** (1980) 971; W. J. Marciano and A. Sirlin, Phys. Rev. **D22** (1980) 2695; Phys. Rev. **D31** (1985) 213(E); A. Sirlin and W. J. Marciano, Nucl. Phys. **B189** (1981) 442; K. I. Aoki et al., Prog. Theor. Phys. Suppl. **73** (1982) 1; M. Bohm, H. Spiesberger and W. Hollik, Forts. Phys. **34** (1986) 1; W. Hollik, Forts. Phys. **38** (1990) 3.
- [22] A. Denner, Fortsch. Phys. **41** (1993) 307.
- [23] R. Santos and A. Barroso, Phys. Rev. **D56** (1997) 5366.
- [24] J. Guasch, J. Sola, W. Hollik, Phys. Lett. **B437** (1998) 88; H. Eberl, S. Kraml, W. Majerotto, JHEP **9905** (1999) 016.
- [25] A. Mendez and A. Pomarol, Phys. Lett. **B279** (1992) 98; L. G. Jin, C. S. Li, Phys.Rev. **D65** (2002) 035007.
- [26] J. Hewett, J. D. Wells, Phys. Rev. **D55** (1997) 5549.
- [27] M. Carena, M. Quiros and C. E. M. Wagner, Nucl. Phys. **B461** (1996) 407; M. Carena, H. E. Haber, S. Heinemeyer, W. Hollik, C. E. M. Wagner, and G. Weiglein, Nucl. Phys. **B580** (2000) 29.
- [28] K. Hagiwara *et al.*, Particle Data Group, Phys. Rev. **D66** (2002) 010001.
- [29] M. Drees and K. Hagiwara, Phys. Rev. **D42** (1990) 1709; M. Drees, K. Hagiwara and A. Yamada, Phys. Rev. **D45** (1992) 1725; P. Chankowski *et al.*, Nucl. Phys. **B417** (1994) 101; D. Garcia and J. Solà, Mod. Phys. Lett. **A9** (1994) 211; A. Djouadi *et al.*, Phys. Rev. Lett. **78** (1997) 3626.
- [30] M. Carena, S. Heinemeyer, C. E. M. Wagner, G. Weiglein, arXiv:hep-ph/9912223.
- [31] Y. You, W. -G. Ma, H. Chen, R. -Y. Zhang, Y. -B. Sun, H. -S. Hou, arXiv:hep-ph/0306036.
- [32] G. Belanger, F. Boudjema, J. Fujimoto, T. Ishikawa, T. Kaneko, K. Kato, Y. Shimizu and Y. Yasui, arXiv:hep-ph/0307029.
- [33] A. Denner, S. Dittmaier, M. Roth, M. M. Weber, arXiv:hep-ph/0307193.
- [34] H. E. Haber and G. L. Kane, Phys. Rep. **117** (1985) 75.

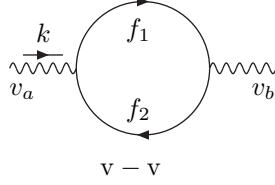


Figure 2: Gauge boson self-energy ($v_a v_b$).

Appendix

In this Appendix, we present the irreducible self-energy and vertex contributions. The convention, Feynman rules, and coupling constants agree with Ref. [34]. In the formulae followed, we have employed Passarino–Veltman one-loop functions B_i , B_{ij} , ($i = 0, 1$) C_i , C_{ij} , C_{ijk} ($i, j, k = 0, 1, 2$) [20] and our notations agree with FeynCalc.

The unrenormalized gauge boson–gauge boson $v_a v_b$ ($v_a v_b = w^- w^-, \gamma\gamma, \gamma z, z z$) self-energies as shown in **Fig. 2** are as follow, which we only extract terms proportional to $m_{t,b}^2$.

$$\begin{aligned}
\Sigma^{v_a v_b} &= -i\Sigma_T^{v_a v_b}(k^2)g_{\mu\nu} - i\Sigma_L^{v_a v_b}(k^2)k_\mu k_\nu \\
\Sigma_T^{ww}(k^2) &= -\frac{g^2 N_c}{48\pi^2}[-m_t^2 - m_b^2 + 2A_0(m_t^2) + m_b^2 B_0(k^2, m_b^2, m_t^2) + (m_t^2 - m_b^2)B_1(k^2, m_b^2, m_t^2)] \\
\frac{\partial \Sigma_T^{ww}(k^2)}{\partial k^2} &= -\frac{g^2 N_c}{96\pi^2 k^2}[-(m_t^2 - m_b^2)(B_0 + 2B_1) + ((m_t^2 - m_b^2)^2 + k^2(m_t^2 + m_b^2))B'_0](k^2, m_b^2, m_t^2) \\
\Sigma_L^{ww}(k^2) &= -\frac{g^2 N_c}{48\pi^2 k^2}[m_t^2 + m_b^2 - 2A_0(m_t^2) + 2m_b^2 B_0(k^2, m_b^2, m_t^2) - 4(m_t^2 - m_b^2)B_1(k^2, m_b^2, m_t^2)] \\
\Sigma_T^{v_a v_b}(k^2) &= -\frac{N_c}{24\pi^2}[2(G_{\bar{q}q}^{Lv_a} G_{\bar{q}q}^{Lv_b} + G_{\bar{q}q}^{Rv_a} G_{\bar{q}q}^{Rv_b})(m_q^2 - A_0(m_q^2)) \\
&\quad - (G_{\bar{q}q}^{Lv_a}(G_{\bar{q}q}^{Lv_b} - 3G_{\bar{q}q}^{Rv_b}) + G_{\bar{q}q}^{Rv_a}(G_{\bar{q}q}^{Rv_b} - 3G_{\bar{q}q}^{Lv_b}))m_q^2 B_0(k^2, m_q^2, m_q^2)] \\
\frac{\partial \Sigma_T^{v_a v_b}(k^2)}{\partial k^2} &= -\frac{N_c}{24\pi^2 k^2}[(G_{\bar{q}q}^{Lv_a} G_{\bar{q}q}^{Lv_b} + G_{\bar{q}q}^{Rv_a} G_{\bar{q}q}^{Rv_b})(-A_0(m_q^2) + m_q^2(1 + B_0(k^2, m_q^2, m_q^2))) \\
&\quad + 3(G_{\bar{q}q}^{Lv_a} G_{\bar{q}q}^{Rv_b} + G_{\bar{q}q}^{Rv_a} G_{\bar{q}q}^{Lv_b})m_q^2 k^2 B'_0(k^2, m_q^2, m_q^2)] \\
\Sigma_L^{v_a v_b}(k^2) &= \frac{N_c}{12\pi^2 k^2}[(G_{\bar{q}q}^{Lv_a} G_{\bar{q}q}^{Lv_b} + G_{\bar{q}q}^{Rv_a} G_{\bar{q}q}^{Rv_b})(-A_0(m_q^2) + m_q^2(1 + B_0(k^2, m_q^2, m_q^2)))] \tag{18}
\end{aligned}$$

with $q = t, b$.

In order to renormalize the Higgs sector, we need to calculate T_s ($s = h, H$), which is the summation of the contribution of two tadpole diagrams in **Fig. 3** (a) and (b), $T_s = T_s^{(a)} + T_s^{(b)}$, where $T_s^{(a)}$, $T_s^{(b)}$ are expressed as

$$\begin{aligned}
T_s^{(a)} &= -i\frac{N_c}{8\pi^2}(G_{ff}^{Ls} + G_{ff}^{Rs})m_f A_0(m_f^2) \\
T_s^{(b)} &= i\frac{N_c}{16\pi^2}G_{s_1 s_1}^s A_0(m_{s_1}^2) \tag{19}
\end{aligned}$$

with $f = t, b$ and $s_1 = \tilde{t}_i, \tilde{b}_i$ ($i = 1, 2$).

The unrenormalized Higgs boson–Higgs boson $s_a s_b$ ($s_a s_b = hh, hH, HH, GG, GA, AA$) self-energies are the summation of contribution shown in **Fig. 4** a, b and c.

$$\Sigma^{s_a s_b} = i\Sigma^{s_a s_b}(k^2) = i(\Sigma_{(a)}^{s_a s_b}(k^2) + \Sigma_{(b)}^{s_a s_b}(k^2) + \Sigma_{(c)}^{s_a s_b}(k^2)) \tag{20}$$

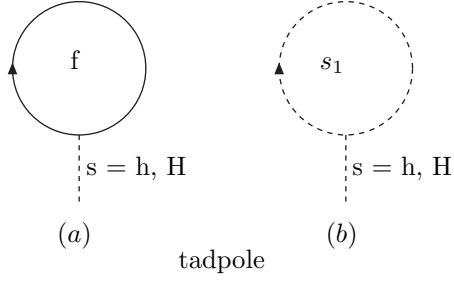


Figure 3: Tadpole diagrams with $s = h, H$.

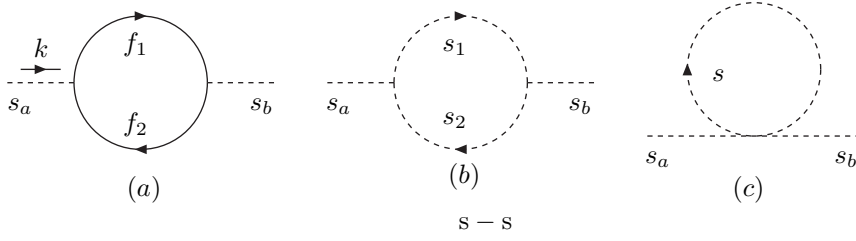


Figure 4: Higgs boson self-energy ($s_a s_b$).

with

$$\begin{aligned}
 \Sigma_{(a)}^{s_a s_b}(k^2) &= \frac{N_c}{48\pi^2} [6(G_{\tilde{f}_1 f_2}^{L s_a} G_{\tilde{f}_2 f_1}^{L s_b} + G_{\tilde{f}_1 f_2}^{R s_a} G_{\tilde{f}_2 f_1}^{R s_b}) m_{f_1} m_{f_2} B_0 \\
 &\quad + (G_{\tilde{f}_1 f_2}^{R s_a} G_{\tilde{f}_2 f_1}^{L s_b} + G_{\tilde{f}_1 f_2}^{L s_a} G_{\tilde{f}_2 f_1}^{R s_b}) (24B_{00} + 6(B_1 + B_{11})k^2)](k^2, m_{f_1}^2, m_{f_2}^2) \\
 \Sigma_{(b)}^{s_a s_b}(k^2) &= -\frac{N_c}{16\pi^2} G_{s_1 s_2}^{s_a} G_{s_2 s_1}^{s_b} B_0(k^2, m_{s_1}^2, m_{s_2}^2) \\
 \Sigma_{(c)}^{s_a s_b}(k^2) &= i \frac{N_c}{16\pi^2} G_{ss}^{s_a s_b} A_0(m_s^2)
 \end{aligned} \tag{21}$$

where $f_1 f_2 = tt, bb$, $s_1 s_2 = \tilde{t}_i \tilde{t}_j, \tilde{b}_i \tilde{b}_j$, and $s = \tilde{t}_i, \tilde{b}_i$ ($i, j = 1, 2$).

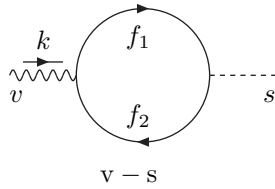


Figure 5: Gauge boson–Higgs boson mixing (vs).

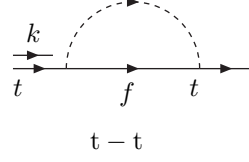


Figure 6: Top quark self-energy.

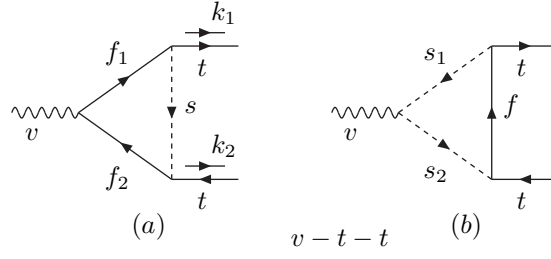


Figure 7: Gauge boson-top quark-top quark vertex (vtt).

The unrenormalized gauge boson-Higgs boson mixing ($vs = zG, zA$) in **Fig. 5** are expressed as

$$\Sigma^{vs} = ik_\mu \Sigma^{vs}(k^2) \quad (22)$$

with

$$\begin{aligned} \Sigma^{vs}(k^2) = & -\frac{N_c}{8\pi^2} [(G_{f_1 f_2}^{Lv} G_{f_2 f_1}^{Rs} + G_{f_1 f_2}^{Rv} G_{f_2 f_1}^{Ls}) m_{f_1} (B_0 + B_1) \\ & + (G_{f_1 f_2}^{Lv} G_{f_2 f_1}^{Ls} + G_{f_1 f_2}^{Rv} G_{f_2 f_1}^{Rs}) m_{f_2} B_1] (k^2, m_{f_1}^2, m_{f_2}^2) \end{aligned} \quad (23)$$

where $f_1 f_2 = tt, bb$.

The unrenormalized top quark self-energy shown in **Fig. 6** are expressed as

$$\Sigma^{tt} = i[\Sigma_L^t(k^2) \not{k} P_L + \Sigma_R^t(k^2) \not{k} P_R + \Sigma_S^t(k^2)] \quad (24)$$

with

$$\begin{aligned} \Sigma_S^t(k^2) &= -\frac{1}{16\pi^2} G_{tf}^{Ls} G_{ft}^{Ls} m_f B_0(k^2, m_f^2, m_s^2) \\ \Sigma_L^t(k^2) &= \frac{1}{16\pi^2} G_{tf}^{Rs} G_{ft}^{Ls} B_1(k^2, m_f^2, m_s^2) \\ \Sigma_R^t(k^2) &= \frac{1}{16\pi^2} G_{tf}^{Ls} G_{ft}^{Rs} B_1(k^2, m_f^2, m_s^2) \end{aligned} \quad (25)$$

where $fs = th, tH, tG, tA, bG^+, bH^+, \tilde{\chi}_i^+ \tilde{b}_\alpha, \tilde{\chi}_j^0 \tilde{t}_\alpha$, ($i, \alpha = 1, 2, j = 1, 2, 3, 4$).

The unrenormalized gauge boson–top quark–top quark vertex ($vtt = \gamma tt, Ztt$) shown in **Fig. 7** (a) and (b) are

$$\begin{aligned} \Gamma^{\text{vtt}} = & \Gamma_1^L k_{1\mu} P_L + \Gamma_2^L k_{2\mu} P_L + \Gamma_3^L \gamma_\mu P_L + \Gamma_4^L \not{k}_1 k_{1\mu} P_L + \Gamma_5^L \not{k}_1 k_{2\mu} P_L + \Gamma_6^L \not{k}_2 k_{1\mu} P_L + \\ & \Gamma_7 \not{k}_2 k_{2\mu} P_L + \Gamma_8^L \not{k}_1 \gamma_\mu P_L + \Gamma_9^L \not{k}_2 \gamma_\mu P_L + \Gamma_{10}^L \not{k}_1 \not{k}_2 \gamma_\mu P_L + (L \rightarrow R) \end{aligned} \quad (26)$$

where $\Gamma_i^{L,R}$ ($i = 1, 2, \dots, 10$) is the summation of $\Gamma_{i(a)}^{L,R}$ and $\Gamma_{i(b)}^{L,R}$, $\Gamma_i^{L,R} = \Gamma_{i(a)}^{L,R} + \Gamma_{i(b)}^{L,R}$, where $\Gamma_{i(a)}^L$ and $\Gamma_{i(b)}^L$ are expressed as follow, and we get $\Gamma_{i(a,b)}^R$ through the exchange of ($L \leftrightarrow R$) in the expressions of corresponding $\Gamma_{i(a,b)}^L$.

$$\begin{aligned} \Gamma_{1(a)}^L &= \frac{1}{8\pi^2} G_{\bar{f}_1 f_2}^{Rv} G_{\bar{t} f_1}^{Ls} G_{\bar{f}_2 t}^{Ls} m_{f_1} C_2 \\ \Gamma_{2(a)}^L &= -\frac{1}{8\pi^2} G_{\bar{f}_1 f_2}^{Rv} G_{\bar{t} f_1}^{Ls} G_{\bar{f}_2 t}^{Ls} m_{f_1} (C_0 + C_1) \\ \Gamma_{3(a)}^L &= \frac{1}{32\pi^2} G_{\bar{t} f_1}^{Rs} G_{\bar{f}_2 t}^{Ls} (2G_{\bar{f}_1 f_2}^{Lv} m_{f_1} m_{f_2} C_0 - G_{\bar{f}_1 f_2}^{Rv} (4C_{00} + 2(C_2 + C_{22})k_1^2 - \\ & \quad 4C_{12}k_1 \cdot k_2 + 2(C_1 + C_{11})k_2^2)) \\ \Gamma_{4(a)}^L &= \frac{1}{8\pi^2} G_{\bar{f}_1 f_2}^{Rv} G_{\bar{t} f_1}^{Rs} G_{\bar{f}_2 t}^{Ls} (C_2 + C_{22}) \\ \Gamma_{5(a)}^L &= -\frac{1}{8\pi^2} G_{\bar{f}_1 f_2}^{Rv} G_{\bar{t} f_1}^{Rs} G_{\bar{f}_2 t}^{Ls} (C_0 + C_1 + C_{12} + C_2) \\ \Gamma_{6(a)}^L &= -\frac{1}{8\pi^2} G_{\bar{f}_1 f_2}^{Rv} G_{\bar{t} f_1}^{Rs} G_{\bar{f}_2 t}^{Ls} C_{12} \\ \Gamma_{7(a)}^L &= \frac{1}{8\pi^2} G_{\bar{f}_1 f_2}^{Rv} G_{\bar{t} f_1}^{Rs} G_{\bar{f}_2 t}^{Ls} (C_1 + C_{11}) \\ \Gamma_{8(a)}^L &= \frac{1}{16\pi^2} G_{\bar{t} f_1}^{Ls} G_{\bar{f}_2 t}^{Ls} (G_{\bar{f}_1 f_2}^{Lv} m_{f_2} C_0 - G_{\bar{f}_1 f_2}^{Rv} m_{f_1} C_2 + G_{\bar{f}_1 f_2}^{Lv} m_{f_2} C_2) \\ \Gamma_{9(a)}^L &= \frac{1}{16\pi^2} G_{\bar{t} f_1}^{Ls} G_{\bar{f}_2 t}^{Ls} (G_{\bar{f}_1 f_2}^{Rv} m_{f_1} C_0 + G_{\bar{f}_1 f_2}^{Rv} m_{f_1} C_1 - G_{\bar{f}_1 f_2}^{Lv} m_{f_2} C_1) \\ \Gamma_{10(a)}^L &= \frac{1}{16\pi^2} G_{\bar{f}_1 f_2}^{Rv} G_{\bar{t} f_1}^{Rs} G_{\bar{f}_2 t}^{Ls} (C_0 + C_1 + C_2) \\ \Gamma_{1(b)}^L &= -\frac{1}{16\pi^2} G_{s_2 s_1}^v G_{\bar{t} f}^{Ls_1} G_{\bar{f} t}^{Ls_2} m_f (C_0 + 2C_2) \\ \Gamma_{2(b)}^L &= \frac{1}{16\pi^2} G_{s_2 s_1}^v G_{\bar{t} f}^{Ls_1} G_{\bar{f} t}^{Ls_2} m_f (C_0 + 2C_1) \\ \Gamma_{3(b)}^L &= \frac{1}{8\pi^2} G_{s_2 s_1}^v G_{\bar{t} f}^{Rs_1} G_{\bar{f} t}^{Ls_2} C_{00} \\ \Gamma_{4(b)}^L &= \frac{1}{16\pi^2} G_{s_2 s_1}^v G_{\bar{t} f}^{Rs_1} G_{\bar{f} t}^{Ls_2} (C_2 + 2C_{22}) \\ \Gamma_{5(b)}^L &= -\frac{1}{16\pi^2} G_{s_2 s_1}^v G_{\bar{t} f}^{Rs_1} G_{\bar{f} t}^{Ls_2} (2C_{12} + C_2) \\ \Gamma_{6(b)}^L &= -\frac{1}{16\pi^2} G_{s_2 s_1}^v G_{\bar{t} f}^{Rs_1} G_{\bar{f} t}^{Ls_2} k_{1\mu} (C_1 + 2C_{12}) \\ \Gamma_{7(b)}^L &= \frac{1}{16\pi^2} G_{s_2 s_1}^v G_{\bar{t} f}^{Rs_1} G_{\bar{f} t}^{Ls_2} (C_1 + 2C_{11}) \\ \Gamma_{8(b)}^L &= 0 \\ \Gamma_{9(b)}^L &= 0 \\ \Gamma_{10(b)}^L &= 0 \end{aligned} \quad (27)$$

with the arguments of the C function as $C(k_2^2, (k_1+k_2)^2, k_1^2, m_s^2, m_{f_2}^2, m_{f_1}^2)$ and $C(k_2^2, (k_1+k_2)^2, k_1^2, m_f^2, m_{s_2}^2, m_{s_1}^2)$ for **Fig. 7** (a) and (b) respectively. For both vertex γtt and Ztt , the virtual particles propagated in the loops are

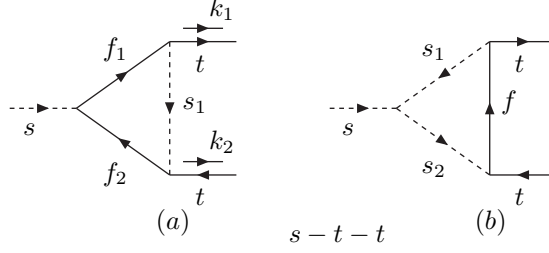


Figure 8: Higgs boson-top quark-top quark vertex (stt).

as follow, $f_1 f_2 s = tth, ttH, ttG, ttA, bbG^-, bbH^-, f s_1 s_2 = bG^-G^-, bH^-H^-$, and additionally $f_1 f_2 s = \tilde{\chi}_i^+ \tilde{\chi}_i^+ \tilde{b}_\alpha^*$, $f s_1 s_2 = \tilde{\chi}_i^+ \tilde{b}_\alpha^* \tilde{b}_\alpha^*, \tilde{\chi}_k^0 \tilde{t}_\alpha^* \tilde{t}_\alpha^*$ for γtt vertex, $f_1 f_2 s = \tilde{\chi}_i^+ \tilde{\chi}_j^+ \tilde{b}_\alpha^*, \tilde{\chi}_k^0 \tilde{\chi}_l^0 \tilde{t}_\alpha^*$, $f s_1 s_2 = thA, tAh, tHA, tAH, thG, tGh, tHG, tGH, \tilde{\chi}_i^+ \tilde{b}_\alpha^* \tilde{b}_\beta^*, \tilde{\chi}_k^0 \tilde{t}_\alpha^* \tilde{t}_\beta^*$ for Ztt vertex, with $i, j = 1, 2, \alpha, \beta = 1, 2, k, l = 1, 2, 3, 4$.

The unrenormalized Higgs boson-top quark-top quark ($stt = htt, Gtt, Att$) vertex shown in **Fig. 8** (a) and (b) are

$$\Gamma^{\text{stt}} = \Gamma_1^L P_L + \Gamma_2^L \not{k}_1 P_L + \Gamma_3^L \not{k}_2 P_L + \Gamma_4^L \not{k}_1 \not{k}_2 P_L + (L \rightarrow R) \quad (28)$$

where $\Gamma_i^{L,R}$ ($i = 1, 2, 3, 4$) is the summation of $\Gamma_{i(a)}^{L,R}$ and $\Gamma_{i(b)}^{L,R}$, $\Gamma_i^{L,R} = \Gamma_{i(a)}^{L,R} + \Gamma_{i(b)}^{L,R}$, where $\Gamma_{i(a)}^L$ and $\Gamma_{i(b)}^L$ are expressed as follow, and we get $\Gamma_{i(a,b)}^R$ through the exchange of ($L \leftrightarrow R$) in the expressions of corresponding $\Gamma_{i(a,b)}^L$.

$$\begin{aligned} \Gamma_{1(a)}^L &= \frac{1}{32\pi^2} G_{\tilde{t}f_1}^{Ls_1} G_{\tilde{f}_2}^{Ls_1} (2G_{\tilde{f}_1 f_2}^{Ls} m_{f_1} m_{f_2} C_0 + G_{\tilde{f}_1 f_2}^{Rs} (8C_{00} + 2(C_2 + C_{22})k_1^2 - \\ &\quad 4C_{12}k_1 \cdot k_2 + 2(C_1 + C_{11})k_2^2)) \\ \Gamma_{2(a)}^L &= \frac{1}{16\pi^2} G_{\tilde{t}f_1}^{Rs_1} G_{\tilde{f}_2}^{Ls_1} (G_{\tilde{f}_1 f_2}^{Ls} m_{f_2} C_0 + G_{\tilde{f}_1 f_2}^{Rs} m_{f_1} C_2 + G_{\tilde{f}_1 f_2}^{Ls} m_{f_2} C_2) \\ \Gamma_{3(a)}^L &= -\frac{1}{16\pi^2} G_{\tilde{t}f_1}^{Rs_1} G_{\tilde{f}_2}^{Ls_1} (G_{\tilde{f}_1 f_2}^{Rs} m_{f_1} C_0 + G_{\tilde{f}_1 f_2}^{Rs} m_{f_1} C_1 + G_{\tilde{f}_1 f_2}^{Ls} m_{f_2} C_1) \\ \Gamma_{4(a)}^L &= -\frac{1}{16\pi^2} G_{\tilde{f}_1 f_2}^{Rs} G_{\tilde{t}f_1}^{Ls_1} G_{\tilde{f}_2}^{Ls_1} (C_0 + C_1 + C_2) \\ \Gamma_{1(b)}^L &= \frac{1}{16\pi^2} G_{s_2 s_1}^s G_{\tilde{t}f}^{Ls_1} G_{\tilde{f}_t}^{Ls_2} m_f C_0 \\ \Gamma_{2(b)}^L &= -\frac{1}{16\pi^2} G_{s_2 s_1}^s G_{\tilde{t}f}^{Rs_1} G_{\tilde{f}_t}^{Ls_2} C_2 \\ \Gamma_{3(b)}^L &= \frac{1}{16\pi^2} G_{s_2 s_1}^s G_{\tilde{t}f}^{Rs_1} G_{\tilde{f}_t}^{Ls_2} C_1 \\ \Gamma_{4(b)}^L &= 0 \end{aligned} \quad (29)$$

with the arguments of the C function as $C(k_2^2, (k_1+k_2)^2, k_1^2, m_s^2, m_{f_2}^2, m_{f_1}^2)$ and $C(k_2^2, (k_1+k_2)^2, k_1^2, m_f^2, m_{s_2}^2, m_{s_1}^2)$ for **Fig. 8** (a) and (b) respectively. For vertex htt, Gtt and Att , the virtual particles propagated in the loops are as follow, $f_1 f_2 s = tth, ttH, ttG, ttA, bbG^-, bbH^-, \tilde{\chi}_i^+ \tilde{\chi}_j^+ \tilde{b}_\alpha^*, \tilde{\chi}_k^0 \tilde{\chi}_l^0 \tilde{t}_\alpha^*$, $f s_1 s_2 = \tilde{\chi}_i^+ \tilde{b}_\alpha^* \tilde{b}_\alpha^*, \tilde{\chi}_k^0 \tilde{t}_\alpha^* \tilde{t}_\alpha^*$, and additionally $f s_1 s_2 = thh, thH, tHh, tHH, tGG, tGA, tAG, tAA, bG^-G^-, bG^-H^-, bH^-G^-, bH^-H^-$ for htt vertex, $f s_1 s_2 = thA, tAh, tHA, tAH, thG, tGh, tHG, tGH$ for Gtt vertex, and $f s_1 s_2 = thA, tAh, tHA, tAH, thG, tGh, tHG, tGH, bG^-H^-, bH^-G^-$ for Att vertex, with $i, j = 1, 2, \alpha, \beta = 1, 2, k, l = 1, 2, 3, 4$,

The unrenormalized Higgs boson-gauge boson-gauge boson ($sv_\alpha v_\beta = h\gamma\gamma, h\gamma Z, hZZ$) vertex shown in **Fig. 9** (a)-(e) are

$$\Gamma^{\text{sv}_\alpha v_\beta} = \Gamma_1 g_{\mu\nu} + \Gamma_2 k_{1\mu} k_{1\nu} + \Gamma_3 k_{2\mu} k_{2\nu} + \Gamma_4 k_{1\mu} k_{2\nu} + \Gamma_5 k_{2\mu} k_{1\nu} + \Gamma_6 \epsilon^{\mu\nu\sigma\tau} k_{1\sigma} k_{2\tau} \quad (30)$$

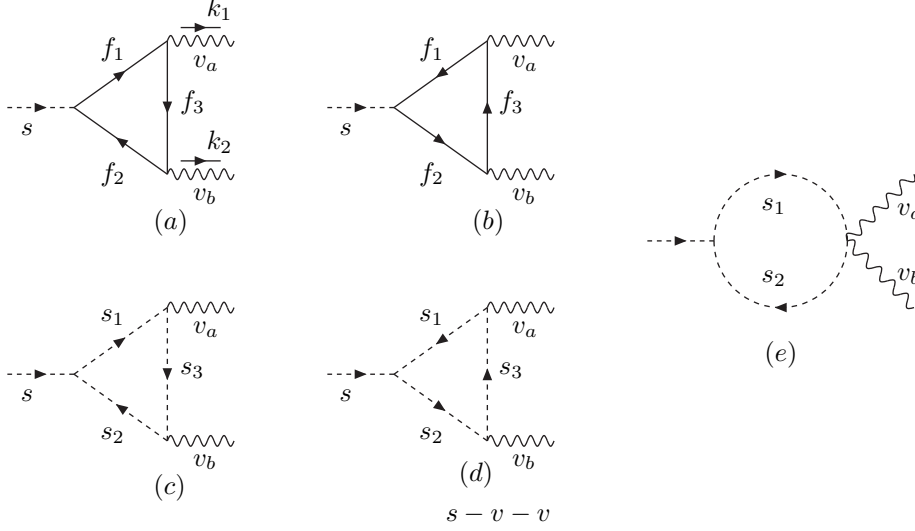


Figure 9: Higgs boson–gauge boson–gauge boson vertex ($sv_a v_b$).

where Γ_i ($i = 1, 2, \dots, 6$) is the summation from $\Gamma_{i(a)}$ to $\Gamma_{i(e)}$, $\Gamma_i = \Gamma_{i(a)} + \Gamma_{i(b)} + \dots + \Gamma_{i(e)}$, where $\Gamma_{i(a)}$, $\Gamma_{i(c)}$ and $\Gamma_{i(e)}$ are expressed as follow,

$$\begin{aligned}
\Gamma_{1(a)} &= \frac{1}{16\pi^2} [-2(G_{\bar{f}_1 f_2}^{Ls} G_{\bar{f}_3 f_1}^{Lv_a} G_{\bar{f}_2 f_3}^{Rv_b} + G_{\bar{f}_1 f_2}^{Rs} G_{\bar{f}_3 f_1}^{Rv_a} G_{\bar{f}_2 f_3}^{Lv_b}) m_{f_1} m_{f_2} m_{f_3} C_0 - (G_{\bar{f}_1 f_2}^{Rs} G_{\bar{f}_3 f_1}^{Lv_a} G_{\bar{f}_2 f_3}^{Lv_b} + G_{\bar{f}_1 f_2}^{Ls} G_{\bar{f}_3 f_1}^{Rv_a} G_{\bar{f}_2 f_3}^{Rv_b}) m_{f_2} \\
&\quad (-4C_{00} - 2(C_2 + C_{22})k_1^2 + 2(C_1 + 2C_{12})k_1 \cdot k_2 - 2C_{11}k_2^2) + \\
&\quad (G_{\bar{f}_1 f_2}^{Rs} G_{\bar{f}_3 f_1}^{Lv_a} G_{\bar{f}_2 f_3}^{Rv_b} + G_{\bar{f}_1 f_2}^{Ls} G_{\bar{f}_3 f_1}^{Rv_a} G_{\bar{f}_2 f_3}^{Lv_b}) m_{f_3} (-8C_{00} - 2(C_2 + C_{22})k_1^2 + \\
&\quad 2(C_0 + C_1 + 2C_{12} + C_2)k_1 \cdot k_2 - 2(C_1 + C_{11})k_2^2) + (G_{\bar{f}_1 f_2}^{Ls} G_{\bar{f}_3 f_1}^{Lv_a} G_{\bar{f}_2 f_3}^{Lv_b} + G_{\bar{f}_1 f_2}^{Rs} G_{\bar{f}_3 f_1}^{Rv_a} G_{\bar{f}_2 f_3}^{Rv_b}) m_{f_1} \\
&\quad (4C_{00} + 2C_{22}k_1^2 - 2(2C_{12} + C_2)k_1 \cdot k_2 + 2(C_1 + C_{11})k_2^2)] \\
\Gamma_{2(a)} &= -\frac{1}{4\pi^2} [(G_{\bar{f}_1 f_2}^{Ls} G_{\bar{f}_3 f_1}^{Lv_a} G_{\bar{f}_2 f_3}^{Lv_b} + G_{\bar{f}_1 f_2}^{Rs} G_{\bar{f}_3 f_1}^{Rv_a} G_{\bar{f}_2 f_3}^{Rv_b}) m_{f_1} C_{22} + (G_{\bar{f}_1 f_2}^{Rs} G_{\bar{f}_3 f_1}^{Lv_a} G_{\bar{f}_2 f_3}^{Lv_b} + G_{\bar{f}_1 f_2}^{Ls} G_{\bar{f}_3 f_1}^{Rv_a} G_{\bar{f}_2 f_3}^{Rv_b}) m_{f_2} (C_2 + C_{22})] \\
\Gamma_{3(a)} &= -\frac{1}{4\pi^2} [(G_{\bar{f}_1 f_2}^{Ls} G_{\bar{f}_3 f_1}^{Lv_a} G_{\bar{f}_2 f_3}^{Lv_b} + G_{\bar{f}_1 f_2}^{Rs} G_{\bar{f}_3 f_1}^{Rv_a} G_{\bar{f}_2 f_3}^{Rv_b}) m_{f_1} (C_1 + C_{11}) + (G_{\bar{f}_1 f_2}^{Rs} G_{\bar{f}_3 f_1}^{Lv_a} G_{\bar{f}_2 f_3}^{Lv_b} + G_{\bar{f}_1 f_2}^{Ls} G_{\bar{f}_3 f_1}^{Rv_a} G_{\bar{f}_2 f_3}^{Rv_b}) m_{f_2} C_{11}] \\
\Gamma_{4(a)} &= \frac{1}{8\pi^2} [(G_{\bar{f}_1 f_2}^{Ls} G_{\bar{f}_3 f_1}^{Lv_a} G_{\bar{f}_2 f_3}^{Lv_b} + G_{\bar{f}_1 f_2}^{Rs} G_{\bar{f}_3 f_1}^{Rv_a} G_{\bar{f}_2 f_3}^{Rv_b}) m_{f_1} (2C_{12} + C_2) + (G_{\bar{f}_1 f_2}^{Rs} G_{\bar{f}_3 f_1}^{Lv_a} G_{\bar{f}_2 f_3}^{Lv_b} + G_{\bar{f}_1 f_2}^{Ls} G_{\bar{f}_3 f_1}^{Rv_a} G_{\bar{f}_2 f_3}^{Rv_b}) m_{f_2} \\
&\quad (C_1 + 2C_{12}) + (G_{\bar{f}_1 f_2}^{Rs} G_{\bar{f}_3 f_1}^{Lv_a} G_{\bar{f}_2 f_3}^{Rv_b} + G_{\bar{f}_1 f_2}^{Ls} G_{\bar{f}_3 f_1}^{Lv_b} G_{\bar{f}_2 f_3}^{Rv_a}) m_{f_3} (C_0 + C_1 + C_2)] \\
\Gamma_{5(a)} &= \frac{1}{8\pi^2} [(G_{\bar{f}_1 f_2}^{Ls} G_{\bar{f}_3 f_1}^{Lv_a} G_{\bar{f}_2 f_3}^{Lv_b} + G_{\bar{f}_1 f_2}^{Rs} G_{\bar{f}_3 f_1}^{Rv_a} G_{\bar{f}_2 f_3}^{Rv_b}) m_{f_1} (2C_{12} + C_2) + (G_{\bar{f}_1 f_2}^{Rs} G_{\bar{f}_3 f_1}^{Lv_a} G_{\bar{f}_2 f_3}^{Lv_b} + G_{\bar{f}_1 f_2}^{Ls} G_{\bar{f}_3 f_1}^{Rv_a} G_{\bar{f}_2 f_3}^{Rv_b}) m_{f_2} \\
&\quad (C_1 + 2C_{12}) - (G_{\bar{f}_1 f_2}^{Rs} G_{\bar{f}_3 f_1}^{Lv_a} G_{\bar{f}_2 f_3}^{Rv_b} + G_{\bar{f}_1 f_2}^{Ls} G_{\bar{f}_3 f_1}^{Lv_b} G_{\bar{f}_2 f_3}^{Rv_a}) m_{f_3} (C_0 + C_1 + C_2)] \\
\Gamma_{6(a)} &= \frac{i}{8\pi^2} [(-G_{\bar{f}_1 f_2}^{Ls} G_{\bar{f}_3 f_1}^{Lv_a} G_{\bar{f}_2 f_3}^{Lv_b} + G_{\bar{f}_1 f_2}^{Rs} G_{\bar{f}_3 f_1}^{Rv_a} G_{\bar{f}_2 f_3}^{Rv_b}) m_{f_1} C_2 + (G_{\bar{f}_1 f_2}^{Rs} G_{\bar{f}_3 f_1}^{Lv_a} G_{\bar{f}_2 f_3}^{Lv_b} - G_{\bar{f}_1 f_2}^{Ls} G_{\bar{f}_3 f_1}^{Rv_a} G_{\bar{f}_2 f_3}^{Rv_b}) m_{f_2} C_1 + \\
&\quad (-G_{\bar{f}_1 f_2}^{Rs} G_{\bar{f}_3 f_1}^{Lv_a} G_{\bar{f}_2 f_3}^{Rv_b} + G_{\bar{f}_1 f_2}^{Ls} G_{\bar{f}_3 f_1}^{Rv_a} G_{\bar{f}_2 f_3}^{Lv_b}) m_{f_3} (C_0 + C_1 + C_2)] \\
\Gamma_{1(c)} &= \frac{1}{4\pi^2} G_{s_3 s_1}^{v_a} G_{s_2 s_3}^{v_b} G_{s_1 s_2}^s C_{00} \\
\Gamma_{2(c)} &= \frac{1}{8\pi^2} G_{s_3 s_1}^{v_a} G_{s_2 s_3}^{v_b} G_{s_1 s_2}^s (C_2 + 2C_{22})
\end{aligned}$$

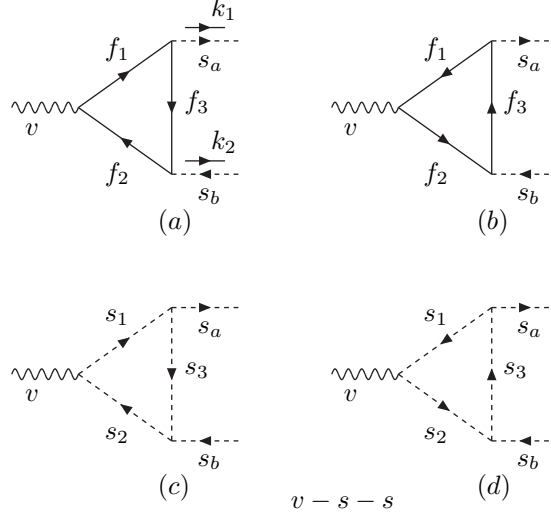


Figure 10: Gauge boson–Higgs boson–Higgs boson vertex ($vs_a s_b$).

$$\begin{aligned}
\Gamma_{3(c)} &= \frac{1}{8\pi^2} G_{s_3 s_1}^{v_a} G_{s_2 s_3}^{v_b} G_{s_1 s_2}^s (C_1 + 2C_{11}) \\
\Gamma_{4(c)} &= -\frac{1}{16\pi^2} G_{s_3 s_1}^{v_a} G_{s_2 s_3}^{v_b} G_{s_1 s_2}^s (C_0 + 2C_1 + 4C_{12} + 2C_2) \\
\Gamma_{5(c)} &= -\frac{1}{4\pi^2} G_{s_3 s_1}^{v_a} G_{s_2 s_3}^{v_b} G_{s_1 s_2}^s C_{12} \\
\Gamma_{6(c)} &= 0 \\
\Gamma_{1(e)} &= -\frac{1}{16\pi^2} G_{s_2 s_1}^{v_a v_b} G_{s_1 s_2}^s B_0((k_1 + k_2)^2, m_{s_1}^2, m_{s_2}^2) \\
\Gamma_{2(e)} &= 0 \\
\Gamma_{3(e)} &= 0 \\
\Gamma_{4(e)} &= 0 \\
\Gamma_{5(e)} &= 0 \\
\Gamma_{6(e)} &= 0
\end{aligned} \tag{31}$$

with arguments of C functions as $C(k_2^2, (k_1 + k_2)^2, k_1^2, m_{f_3}^2, m_{f_2}^2, m_{f_1}^2)$ and $C(k_2^2, (k_1 + k_2)^2, k_1^2, m_{s_3}^2, m_{s_2}^2, m_{s_1}^2)$ for **Fig. 9** (a) and (c), and we get the result of **Fig. 9** (b) and (d) with the exchange of $v_a \leftrightarrow v_b$ and $f, s_1 \leftrightarrow f, s_2$ from the one of **Fig. 9** (a) and (c). For the vertex $h\gamma\gamma, h\gamma Z, hZZ$, the virtual fields propagated in the loops are as follow, $f_1 f_2 f_3 = t\bar{t}, b\bar{b}, \tau\bar{\tau}$ in **Fig. 9** (a), $s_1 s_2 s_3 = \tilde{t}_\alpha \tilde{t}_\beta \tilde{t}_\gamma, \tilde{b}_\alpha \tilde{b}_\beta \tilde{b}_\gamma$ in **Fig. 9** (c), $s_1 s_2 = \tilde{t}_\alpha \tilde{t}_\beta, \tilde{b}_\alpha \tilde{b}_\beta$ in **Fig. 9** (e). Note that γ couples only with scalar quarks of the same quantum numbers, i.e., $\gamma \tilde{t}_\alpha \tilde{t}_\alpha$.

The unrenormalized gauge boson–Higgs boson–Higgs boson ($vs_a s_b = \gamma hG, \gamma hA, ZhG, ZhA$) vertex shown in **Fig. 10** (a)-(d) are

$$\Gamma^{vs_a s_b} = \Gamma_1(k_1 - k_2)_\mu + \Gamma_2(k_1 + k_2)_\mu \tag{32}$$

where $\Gamma_{1,2}$ is the summation from $\Gamma_{i(a)}$ to $\Gamma_{i(d)}$, $\Gamma_i = \Gamma_{i(a)} + \Gamma_{i(b)} + \dots + \Gamma_{i(d)}$, where $\Gamma_{i(a)}$ and $\Gamma_{i(c)}$ are expressed as follow,

$$\Gamma_{1(a)} = \frac{1}{24\pi^2} [-3(G_{f_1 f_2}^{Rv} G_{f_3 f_1}^{Ls_a} G_{f_2 f_3}^{Rs_b} + G_{f_1 f_2}^{Lv} G_{f_3 f_1}^{Rs_a} G_{f_2 f_3}^{Ls_b}) m_{f_1} m_{f_2} (C_1 + C_2) - 3((G_{f_1 f_2}^{Rv} G_{f_3 f_1}^{Ls_a} G_{f_2 f_3}^{Ls_b} + G_{f_1 f_2}^{Lv} G_{f_3 f_1}^{Rs_a} G_{f_2 f_3}^{Rs_b}))$$

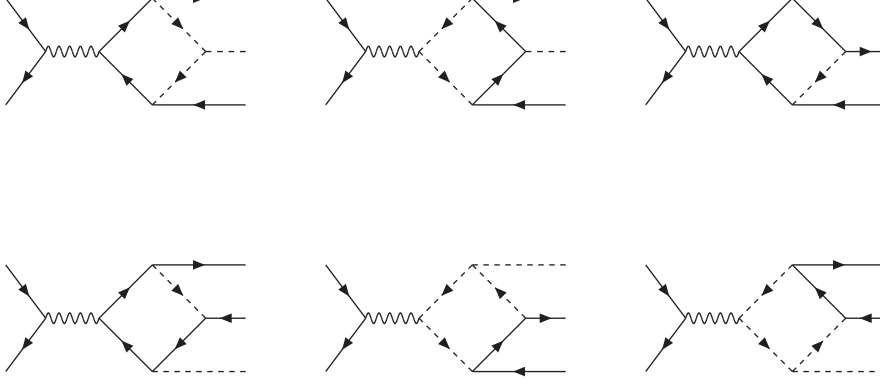


Figure 11: Box diagrams.

$$\begin{aligned}
& m_{f_1} + (G_{\bar{f}_1 f_2}^{Lv} G_{\bar{f}_3 f_1}^{Ls_a} G_{\bar{f}_2 f_3}^{Ls_b} + G_{\bar{f}_1 f_2}^{Rv} G_{\bar{f}_3 f_1}^{Rs_a} G_{\bar{f}_2 f_3}^{Rs_b}) m_{f_2} m_{f_3} (C_0 + C_1 + C_2) - \\
& (G_{\bar{f}_1 f_2}^{Lv} G_{\bar{f}_3 f_1}^{Ls_a} G_{\bar{f}_2 f_3}^{Rs_b} + G_{\bar{f}_1 f_2}^{Rv} G_{\bar{f}_3 f_1}^{Rs_a} G_{\bar{f}_2 f_3}^{Ls_b}) (3(C_2 + 2C_{22} + 2C_{222}) k_1^2 + 2(12C_{00} + 9C_{001} + 9C_{002}) - \\
& 6(C_{112} + 2C_{12} + C_{222}) k_1 \cdot k_2 + 3(C_1 + 2C_{11} + C_{111} + C_{112}) k_2^2) \\
\Gamma_{2(a)} = & \frac{1}{8\pi^2} [(G_{\bar{f}_1 f_2}^{Rv} G_{\bar{f}_3 f_1}^{Ls_a} G_{\bar{f}_2 f_3}^{Rs_b} + G_{\bar{f}_1 f_2}^{Lv} G_{\bar{f}_3 f_1}^{Rs_a} G_{\bar{f}_2 f_3}^{Ls_b}) m_{f_1} m_{f_2} (C_1 - C_2) + (G_{\bar{f}_1 f_2}^{Rv} G_{\bar{f}_3 f_1}^{Ls_a} G_{\bar{f}_2 f_3}^{Ls_b} + G_{\bar{f}_1 f_2}^{Lv} G_{\bar{f}_3 f_1}^{Rs_a} G_{\bar{f}_2 f_3}^{Rs_b}) \\
& m_{f_1} m_{f_3} (C_0 + C_1 - C_2) - (G_{\bar{f}_1 f_2}^{Lv} G_{\bar{f}_3 f_1}^{Ls_a} G_{\bar{f}_2 f_3}^{Ls_b} + G_{\bar{f}_1 f_2}^{Rv} G_{\bar{f}_3 f_1}^{Rs_a} G_{\bar{f}_2 f_3}^{Rs_b}) m_{f_2} m_{f_3} (C_0 - C_1 + C_2) - \\
& (G_{\bar{f}_1 f_2}^{Lv} G_{\bar{f}_3 f_1}^{Ls_a} G_{\bar{f}_2 f_3}^{Rs_b} + G_{\bar{f}_1 f_2}^{Rv} G_{\bar{f}_3 f_1}^{Rs_a} G_{\bar{f}_2 f_3}^{Ls_b}) (-6C_{001} + 6C_{002} - C_2 k_1^2 + 2(C_{112} - C_{222}) k_1 \cdot k_2 + \\
& (C_1 - C_{111} + C_{112}) k_2^2) \\
\Gamma_{1(c)} = & \frac{1}{8\pi^2} G_{s_3 s_1}^{s_a} G_{s_2 s_3}^{s_b} G_{s_1 s_2}^v (C_0 + C_1 + C_2) \\
\Gamma_{2(c)} = & \frac{1}{8\pi^2} G_{s_3 s_1}^{s_a} G_{s_2 s_3}^{s_b} G_{s_1 s_2}^v (-C_1 + C_2) \tag{33}
\end{aligned}$$

with arguments of C functions as $C(k_2^2, (k_1 + k_2)^2, k_1^2, m_{f_3}^2, m_{f_2}^2, m_{f_1}^2)$ and $C(k_2^2, (k_1 + k_2)^2, k_1^2, m_{s_3}^2, m_{s_2}^2, m_{s_1}^2)$ for **Fig. 9 (a)** and **(c)**, and we get the result of **Fig. 10 (b)** and **(d)** with the exchange of $s_a \leftrightarrow s_b$ and $f, s_1 \leftrightarrow f, s_2$ from the one of **Fig. 10 (a)** and **(c)**. For the vertex $\gamma h G_2, \gamma h A, ZhG, ZhA$, the virtual fields propagated in the loops are as follow, $f_1 f_2 f_3 = ttt, bbb, s_1 s_2 s_3 = \tilde{t}_\alpha \tilde{t}_\beta \tilde{t}_\gamma, \tilde{b}_\alpha \tilde{b}_\beta \tilde{b}_\gamma$.

The analytic expressions of box diagrams in **Fig. 11** are too length to present here, while we keep them in our numerical calculation.

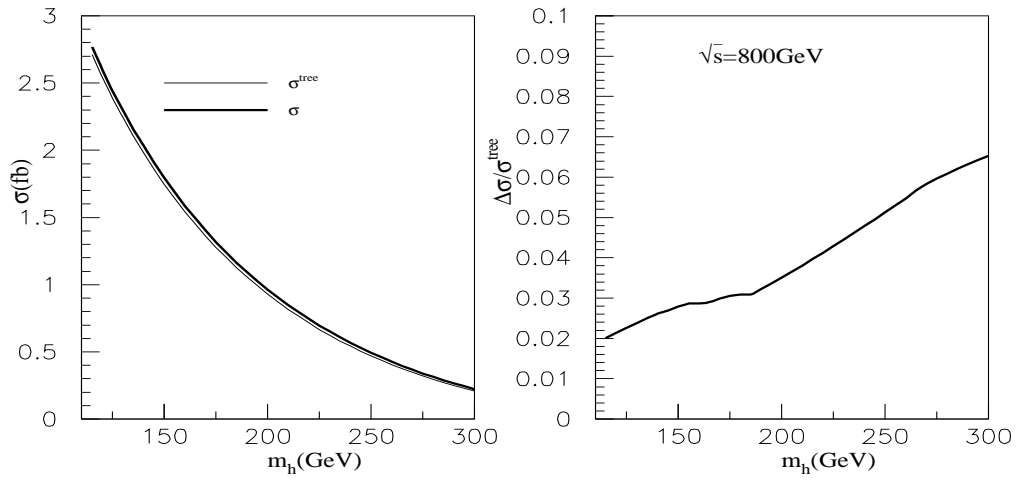


Figure 12: σ (left) and corresponding $\Delta\sigma/\sigma^{\text{tree}}$ (right) as a function of m_h with $\sqrt{s} = 800\text{GeV}$ in the SM.

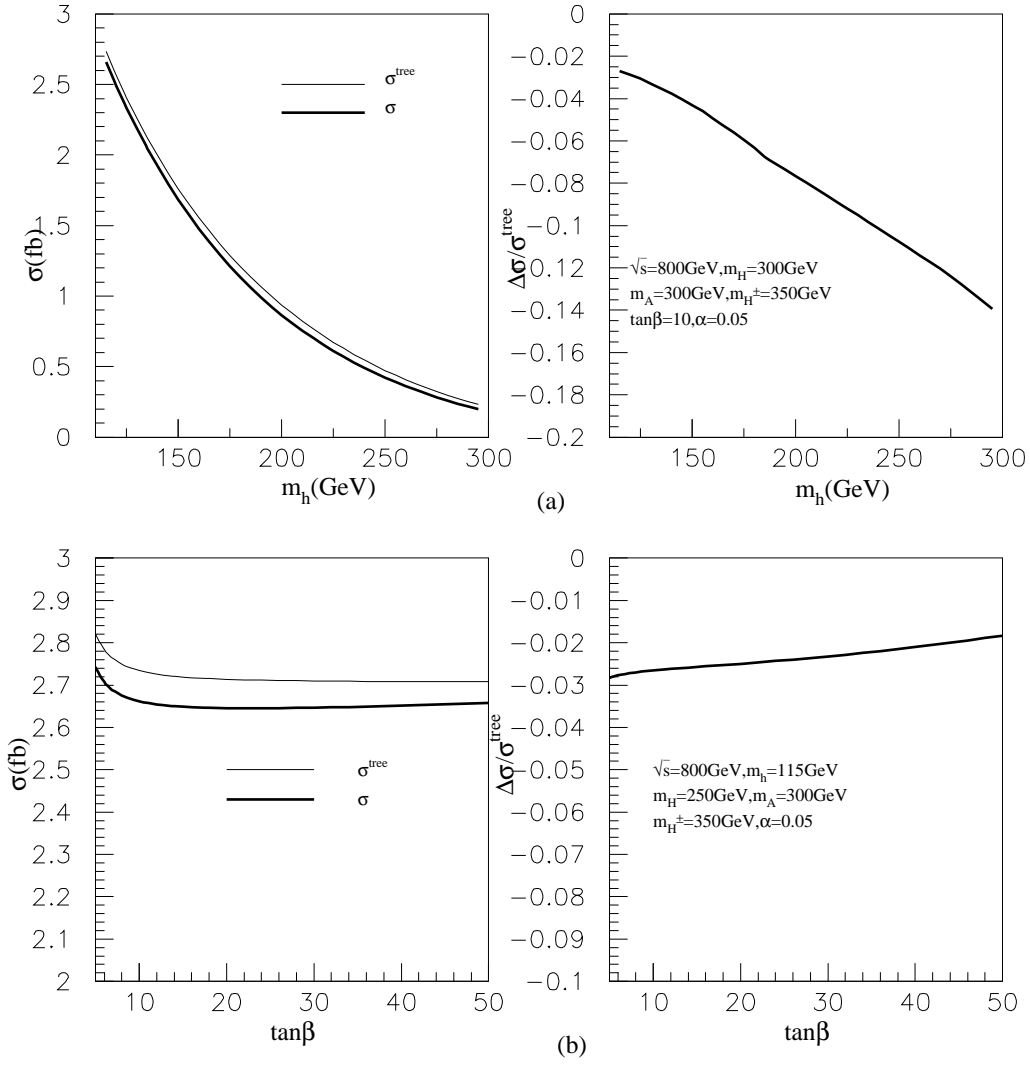


Figure 13: σ (left) and corresponding $\Delta\sigma/\sigma^{\text{tree}}$ (right) as a function of m_h and $\tan\beta$ corresponding respectively to (a), and (b) in 2HDM with $\sqrt{s} = 800\text{ GeV}$.

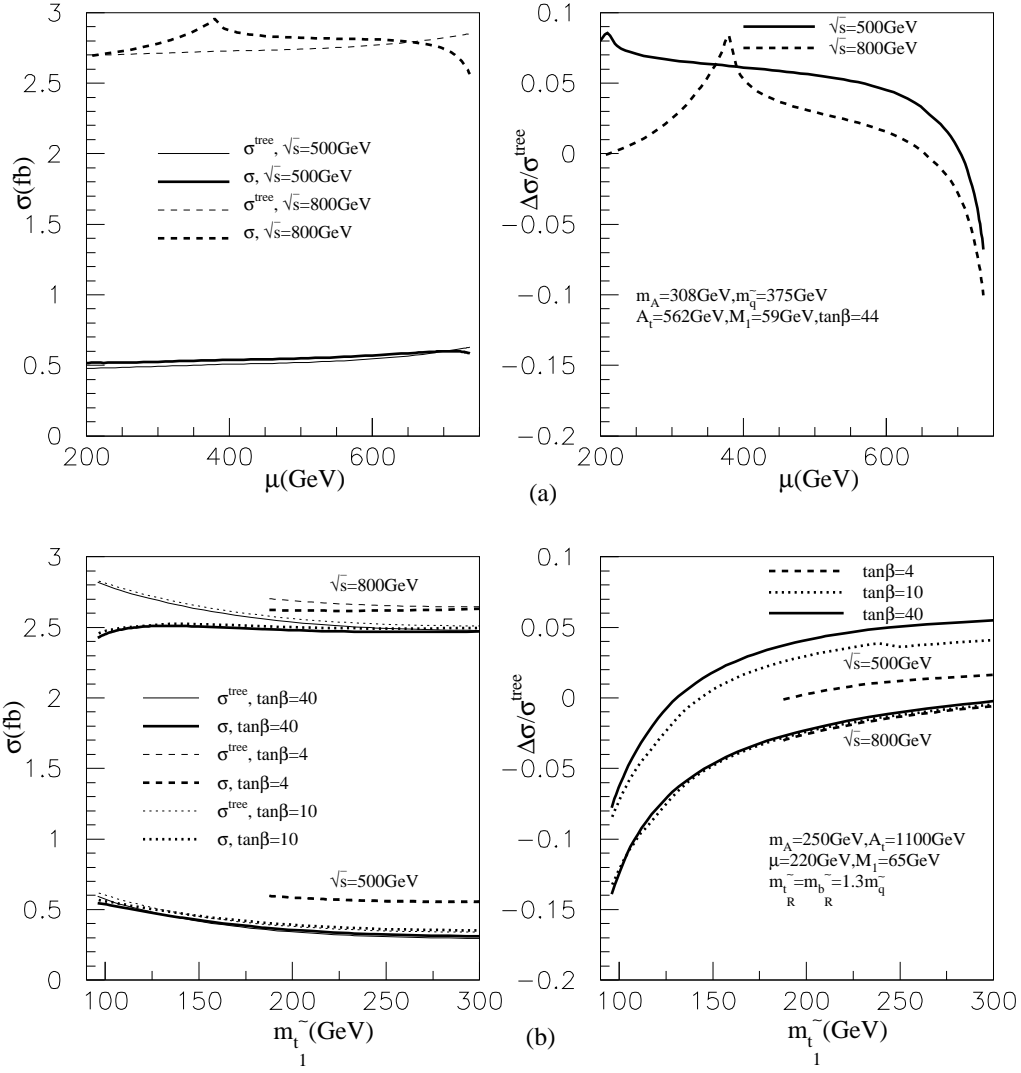


Figure 14: σ (left) and corresponding $\Delta\sigma/\sigma^{\text{tree}}$ (right) as a function of μ and the lightest scalar top quark mass $m_{\tilde{t}_1}$ corresponding respectively to (a) and (b) in MSSM with $\sqrt{s} = 500, 800$ GeV.

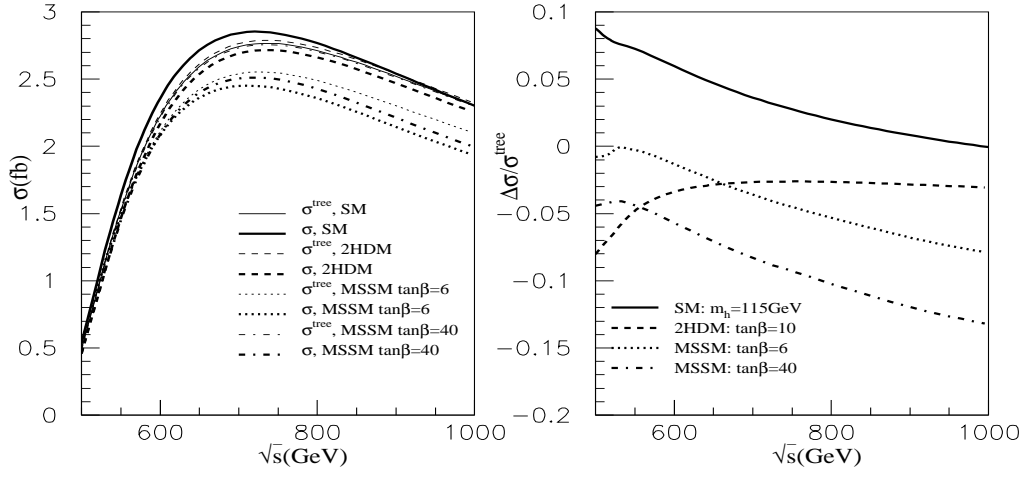


Figure 15: σ (left) and corresponding $\Delta\sigma/\sigma^{\text{tree}}$ (right) as a function of \sqrt{s} in the SM, 2HDM and MSSM. The other 2HDM parameters are $m_h = 115\text{GeV}$, $m_H = 250\text{GeV}$, $m_A = 300\text{GeV}$, $m_{H^\pm} = 350\text{GeV}$, and $\alpha = 0.05$. And the other MSSM parameters are $M_A = 160\text{GeV}$, $A_t = 1\text{TeV}$, $\mu = 220\text{GeV}$, $M_1 = 70\text{GeV}$ and $m_{\tilde{t}_R} = m_{\tilde{b}_R} = 1.5m_{\tilde{q}}$.